JOURNAL OF SPACECRAFT AND ROCKETS
Vol. 42, No. 4, July–August 2005

Fairing Noise Control Using Tube-Shaped Resonators

Steven A. Lane*
U.S. Air Force Research Laboratory, Kirtland Air Force Base, New Mexico 87117
Robert E. Richard†
Boeing–SVS, Albuquerque, New Mexico 87109
and
Scott J. Kennedy‡
CSA Engineering, Albuquerque, New Mexico 87123

The potential for noise mitigation in composite Chamber Core fairings is investigated by using the walls of the fairing structure itself as acoustic resonators. This is the first documented application of long cylindrical tube-shaped resonators for fairing noise control. The theory and modeling of tube-shaped resonators for controlling fairing acoustic resonances is presented. The potential for noise mitigation in composite Chamber Core fairing using the walls of the fairing structure itself as acoustic resonators is investigated. Design criteria such as geometry, damping, spatial coupling, and robustness are considered for a variety of tube resonators. The results showed that a small number of tube resonators reduced the amplitude of low-frequency acoustic resonances by 10–12 dB in the test system and provided nearly 6 dB of reduction over the bandwidth from 0 to 400 Hz.

Introduction

THE Air Force Research Laboratory, Space Vehicles Directorate, is developing a new fabrication approach for composite launch-vehicle fairings, called Chamber Core.[1,2] A Chamber Core structure is fabricated from multilayered composite face sheets separated by channel-shaped chambers as shown in Fig. 1. In addition to providing a strong, lightweight fairing, it is anticipated that the chambers of the structure can be developed into acoustic resonators capable of damping low-frequency acoustic resonances within the fairing. These acoustic resonances are strongly excited by structural vibration and aeroacoustic noise and are difficult to mitigate with passive blanket treatments due to their long wavelengths. Interior noise is a significant problem for lightweight composite fairings, because these structures are usually lightly damped and blanket treatments are minimized to reduce weight and allow the greatest possible payload volume.

Acoustic resonators have been used for noise control in many applications. They are commonly used to reduce noise transmission in ducts, exhaust systems, and aircraft-engine nacelles.[3,4] These systems typically exhibit tonal noise propagation, and the resonators are used as reactive devices to block plane-wave propagation. Acoustic resonators have also been added to sound barriers to improve performance. Noise reduction over a target-frequency bandwidth can be achieved by adding acoustic resonators that have different resonance frequencies. In a study by Kuntz et al., hemispherical resonators were applied to the walls of a propeller aircraft, and the cabin noise was reduced by 11 dB in laboratory tests.[5] Kuntz et al. concluded from their experiments that the resonators increased the transmission loss of double-panel sidewalls at and near the frequency of the resonators. They suggested that resonators could be tuned to the blade-passage frequency of the propeller-driven plane to reduce or prevent the transmission of external noise through the aircraft fuselage.

Received 22 January 2004; revision received 10 June 2004; accepted for publication 22 June 2004.

*Research Aerospace Engineer, Space Vehicles Directorate, 3550 Aberdeen Avenue. Member AIAA.
†Senior Mechanical Engineer, 4411 The 25 Way.
‡Research Scientist, 1300 Britt Street.

In a Chamber Core fairing, as sketched in Fig. 2, the acoustic resonators run parallel to the fairing axis and resemble long tubes. Conceptually, an orifice would be bored through the inner face sheets into the hollow chamber, and a suitable "neck" inserted into the orifice, which permits coupling of the resonator to the internal-fairing acoustic modes. Because of the unconventional geometry of the resulting tube-shaped resonators, they do not behave as classical Helmholtz resonators.[6] The fundamental resonance frequency of a Helmholtz resonator typically has an acoustic wavelength greater than any dimension of the resonator, but in the present case, the desired wavelength of the resonator frequency may approach the length of the resonator. Still, it is necessary to be able to model and predict the frequency and behavior of the tube resonators in order to use them effectively for fairing noise control.

Chanaud conducted a good analysis of the effects of geometry on the resonance frequency of Helmholtz resonators.[7] In that work, an equation for the resonance frequency of Helmholtz resonators was developed from the wave equation and compared to other models that are available in the literature, such as the Rayleigh model and a transcendental equation model. Comparisons were made for a variety of orifice and cavity geometries. That work showed that resonator models have a limited range of validity if the geometry varies significantly. Chanaud showed that resonator behavior is dependent on many variables and showed that there was no simple adjustment or correction that could effectively correct the models. In addition to cavity geometry, Chanaud investigated orifice size, shape, position, and thickness. It was concluded that a computer program must be used to accurately predict the resonance frequency of resonators with unusual geometry.

Selamet et al. published a study in 1995 that investigated the effect on the resonance frequency when the resonator volume's length-to-diameter ratio was changed.[8] They compared models with experimental measurements made with an impedance-tube-type setup. They concluded that volume dimensions have a significant impact on resonance frequency. Furthermore, an increase in the length-to-diameter ratio reduced the resonance frequency, and they compared this phenomenon to the effect of adding a length correction to the neck. They also concluded that the resonance frequency depended on neck dimensions, volume size, and geometry and suggested that a multidimensional computational study would be necessary to accurately model resonators of unusual geometries.

In follow-up work, Dickey and Selamet considered concentric resonators in which the length-to-diameter ratio was small, referred to as a "pancake" configuration.[9] They were able to develop a closed-form analytical expression for the resonance frequency for

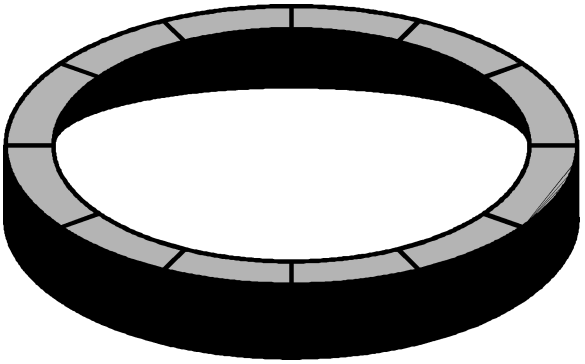

Fig. 1 Cylindrical ring illustrating Chamber Core construction.

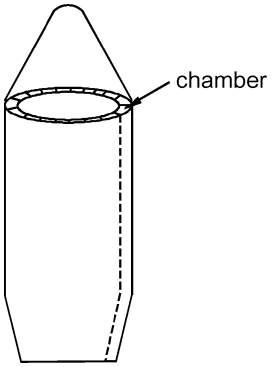

Fig. 2 Illustration of Chamber Core fairing.

this geometry. Their results showed that for extreme geometries, higher-frequency, length-controlled resonances occurred.

The tube-shaped resonators studied in this work have a neck that attaches to the side of the resonator volume and is different from the concentric-type resonators previously studied. To the best of the authors' knowledge, there has been no investigation of tube-shaped resonators for attenuating the modal response in an acoustic enclosure. However, work in this area is under way at the University of Pittsburgh.[10] Tube-shaped resonators investigated here do not follow the classical lumped-parameter models. It was found that tube-shaped resonators more closely resemble quarter-wave resonators in their response characteristics.

Schofield[11] and Fahy and Schofield[12] published theoretical development and modeling of the interaction of an acoustic resonator and an acoustic enclosure in 1979. In their development, they considered both Helmholtz resonators and quarter-wave type resonators. Their work was later extended by Cummings to include an array of resonators in an acoustic volume excited by an arbitrary disturbance.[13] Some of the important results and conclusions will be reiterated, but the development of the analytical model will not be given. Although their models were developed for a reverberant chamber, their conclusions are applicable to the fairing problem, as evidenced by the data presented in this work.

The performance of acoustic resonators depends on their coupling to the acoustic modes to be attenuated, which in turn depends on frequency tuning, damping, and spatial positioning. Modeling of the tube-shaped resonators is presented first. Next, a few notes are given regarding the behavior of acoustic resonators interacting with lightly damped acoustic enclosures. Three resonator designs were tested in an aluminum cylinder that included a flexible structural-acoustic transmission path and an external acoustic source, similar to the actual fairing problem. The effect of single and multiple resonators designed for single and multiple resonances is presented.

Theory

Resonator Modeling

Three different tube-shaped resonator geometries were investigated: L-shaped, T-shaped, and U-shaped tubes. The resonators had a volume ratio consistent with that of an actual Chamber Core fairing. For a 2-m-diam fairing, it was estimated that 4-cm-diam (≈1.5-in.) resonators would be reasonable. Thus, using a constant aspect ratio of fairing diameter to resonator diameter, tube resonators were constructed using 13-mm ($\frac{1}{2}$-in.)-diameter polyvinyl chloride (PVC) pipe for the test cylinder (which was approximately 0.56 m in diameter). The resonator necks were also made using PVC pipe of the same diameter. The ends of the tubes were capped using standard PVC caps.

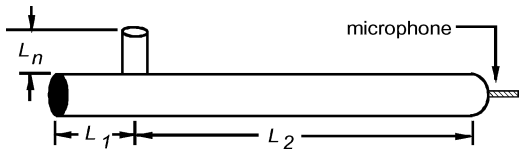

Fig. 3 Schematic of the L-shaped tube resonator.

A schematic of an L-shaped resonator is shown in Fig. 3. If L_1 is small relative to L_2, then it resembles a quarter-wave resonator, except that the orifice, or neck, is positioned on the side of the tube as opposed to concentrically. A classical quarter-wave resonator is simply a pipe with one end open and the other end closed. The closed end creates a reflective boundary (pressure maximum), and the open end creates a "pressure release" (pressure node) boundary. Thus, the wavelength of the fundamental resonance frequency corresponds to four times the length of the tube; hence the name quarter-wave resonator. The mode shape of the fundamental mode looks like a quarter of a cosine curve. Additional information on quarter-wave resonators can be found in Refs. 3 and 6. For a quarter-wave resonator, the resonance frequencies are given by

$$f_n = [(2n - 1)/4](c/L) \tag{1}$$

where L is the tube length, n is the mode number, and c is the speed of sound. This relation was tested and found to predict the frequencies of a quarter-wave resonator made from PVC relatively well, considering that no adjustment was included for losses. To investigate the effect of moving the neck away from the end toward the middle of the tube, the resonance frequency was measured while L_1 and L_2 were varied, but $L_1 + L_2$ were kept constant. Data were taken for a range of neck lengths, L_n, which varied from approximately 6 to 18 cm (2.5–7 in.) (the measurement uncertainty was less than 1.6 mm). Four combinations of L_1 and L_2 with $L_1 + L_2 = 80$ cm were used (9, 71, 23, 57, 31, 49, 37, and 43 cm). (The measurement uncertainty was less than 1.6 mm on these parts.) The measured data showed that the sum of neck length, L_n, and the larger dimension, L_2, determined the fundamental resonance frequency. As predicted in the previous literature, a correction factor on each of these terms improved the prediction of the resonance frequencies. For this particular resonator configuration, a reasonable model for the fundamental resonance frequency, denoted as f_1, was found to be

$$f_1 = c/4L_{\text{eq}} \tag{2}$$

where L_{eq} is

$$L_{\text{eq}} = \alpha L_n + \beta L_2 \tag{3}$$

The parameters α and β were computed by curve fitting (least squares) the measured data and were determined to be $\alpha = 1.9$ and $\beta = 0.9$ for this resonator configuration (computed in Matlab using double precision; three significant figures were carried, but the solution was rounded to two). The speed of sound was assumed to be about 336 m/s (23°C at 1620 m above sea level). For 35 test cases, the measured frequency and model predictions are compared in Fig. 4. The resonance frequency of the tube resonators was determined by inserting a microphone into the tube, L_2. (It is also possible to put the microphone in the neck tube, but care must be taken not to obstruct the flow.) Ambient noise (or generated noise) excited the tube resonances, which the microphone measured. For each case, 20 averages of the microphone autospectrum were taken with a Siglab spectrum analyzer. For the bandwidth and number of points used,

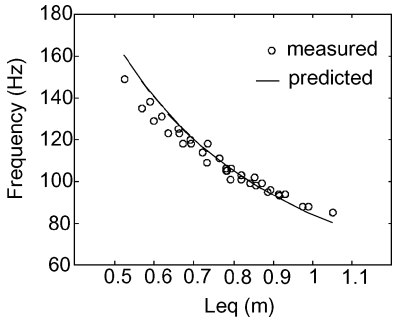

Fig. 4 Model predictions vs experimental measurements for the L-shaped resonator ($L_1 + L_2 = 80$ cm).

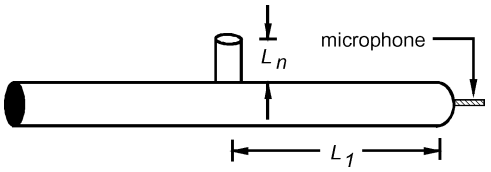

Fig. 5 Schematic of the T-shaped tube resonator.

a frequency resolution of 0.5 Hz was achieved. Measurements with the microphone inserted into L_2 matched measurements with the microphone in the neck.

The model was reasonably accurate given the experimental uncertainty of using PVC materials and not accounting for losses. The model predictions corresponded well for a wide range of neck lengths, neck positions, and resonator frequencies. An advantage of this model is that it does not require information about the various cross-sectional areas. The resonance predicted by classic lumped-parameter models were computed and compared to the measured values, but were off by at least a factor of 2 in most cases.

There are a couple of important observations to be made from these tests. First, as the neck was moved away from the end, it was expected that the tube would behave less like an open-ended quarter-wave resonator and start showing the dynamics of a "closed–closed" tube, but this was not the case. Second, the dimension L_1 did not have an appreciable effect on predicting the resonator frequency. Tests were also conducted, though they are not presented here, that showed that for constant L_n and L_2, when L_1 was allowed to vary from $L_1 = 0.3L_2$ to $L_1 = L_2$, the model remained valid and was not substantially affected by the change in L_1. Finally, the model prediction did not require information regarding the diameter of the neck relative to the diameter of the tube, which probably results from having similar-diameter pipe sections. Future investigations will determine if additional parameterization is needed for cases where tube diameter is significantly different from neck diameter.

T-shaped resonators are a subset of L-shaped resonators, where $L_1 = L_2$ as shown in Fig. 5. Data were measured for a series of tests in which L_n varied from 9 to 18 cm and $L_1 = L_2 = 24$, 29, 33, or 71 cm (measurement uncertainty was less than 1.6 mm). The data were measured using the same method as used for the L-shaped resonators. Using the model given in Eqs. (2) and (3), a curve-fit was performed on the data, and $\alpha = 2.3$ and $\beta = 1.1$ were computed. These values are close to those computed for the L-shaped resonators. A comparison of the measured resonance frequencies and those predicted by the model are shown in Fig. 6. For these tests, there were more cases covering a wider frequency band, which likely accounts for the changes in α and β.

U-shaped resonators are similar to T-shaped resonators in that the neck is between two nearly equal tube lengths as shown in Fig. 7. The U-shaped resonators demonstrate that the tube does not need to be straight, but can be bent at an angle. Measurements of the fundamental and the next two harmonics were made to determine whether the model could be used to predict higher order modes using Eq. (1). Again, the microphone was inserted through a single end cap into the L_2 tube section. The data closely matched measurements taken

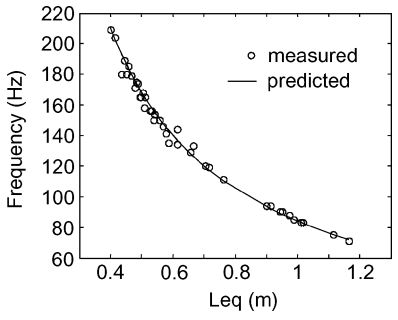

Fig. 6 Model predictions vs experimental measurements for the T-shaped resonator.

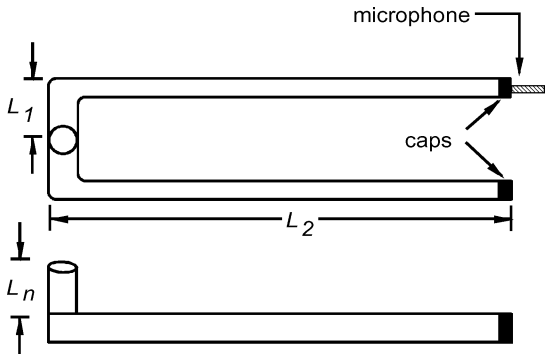

Fig. 7 Schematic of the U-shaped tube resonator.

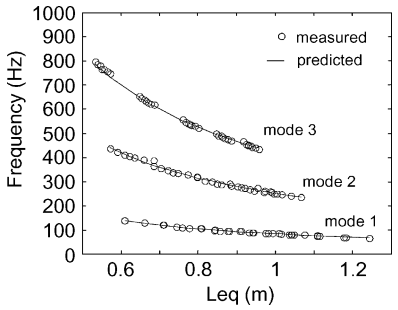

Fig. 8 Model predictions vs experimental measurements for the U-shaped resonator.

with the microphone in the neck tube (±0.3 Hz). The parameters α and β changed for each resonance frequency, but the resulting model predictions agreed with the measurements as shown in Fig. 8. By curve-fitting the measured data, it was found that for the first resonance, $\alpha = 2.6$ and $\beta = 1.0$; for the second resonance, $\alpha = 1.0$ and $\beta = 1.1$; and for the third resonance, $\alpha = 0.3$ and $\beta = 1.1$. Figure 8 shows that once the values of α and β have been determined for a particular resonator, the model can be used to design a resonator for any desired frequency within the range. Thus, we have a relatively simple model that should be useful for designing resonators for the Chamber Core structure.

Controlling Acoustic Resonances

Analogous to tuned mass dampers on a vibrating structure, acoustic resonators can be used to damp the modal response of acoustic enclosures. Schofield[11] and Fahy and Schofield[12] studied the interaction of a single acoustic mode and resonator. They also performed experiments in which an optimally tuned resonator was placed in a reverberant enclosure to target a single room mode. They showed that the optimal damping for narrow-band attenuation about a single acoustic mode is given by

$$\frac{\varepsilon}{\eta_n} = \frac{2(\varepsilon/\eta_r)^3}{1 - (\varepsilon/\eta_r)^2 - (\varepsilon/\eta_r)^4} \tag{4}$$

where ε is the coupling parameter, η_n is the acoustic modal damping, and η_r is the damping of the acoustic resonator. The coupling between the resonator and the acoustic volume is given as

$$\varepsilon^2 = \frac{\rho_0 c_0^2 \varphi_n^2(\boldsymbol{r}_r) S^2}{\omega_c^2 \Lambda_n M} \tag{5}$$

where M/S^2 is the acoustic mass of the system, ω_c is the resonance frequency of both the acoustic mode and the additional resonator, ρ_0 is the density of the fluid, c_0 is the speed of sound in the fluid, Λ_n is the modal volume of mode n, and $\varphi_n(\boldsymbol{r}_r)$ is the value of the mode shape function for mode n at the resonator neck. Their results showed that for a coupled resonator/acoustic system, the effect of the resonator was to split the acoustic resonance of the cavity into two resonance peaks that occurred on either side of the original acoustic resonant frequency. The magnitude of the resulting two peaks was typically less than that of the original, although energy was spread over a greater bandwidth. Also, it is apparent from Eq. (5) that strong coupling can only occur in modes in which the resonator neck (or orifice) is not located at a pressure node, because that would result in the value of the mode shape going to zero.

Cummings expanded this work to a multimode acoustic system and analyzed the effects of multiple resonators using numerical simulations.[13] He addressed the issue of coupling to multiple acoustic modes with a single acoustic resonator. His research showed that in high-modal-density acoustic systems, a single resonator was able to couple with multiple resonances. Furthermore, Cummings observed that for widely spaced acoustic modes (i.e., separated by a range of frequencies so that each mode is clearly distinguishable), two resonators designed for different modes have little influence upon each other. The reason was that the impedance of a single resonator becomes large away from its resonant frequency and therefore couples weakly to the acoustic field or other resonators.

In addition to the position of the resonator orifice relative to the acoustic-pressure nodes, Eq. (4) indicates the strong dependence of resonator performance on the damping of the resonator and the acoustic system. It has been noted that a resonator will split an acoustic-resonance peak into two lesser amplitude peaks. However, if damping is added to the resonator, the two resulting peaks can be further reduced in amplitude, creating a smooth plateau effect referred to as "optimal" by Fahy and Schofield.[12] Also, excessive damping can reduce coupling and thereby reduce performance. Cummings noted that for lightly damped resonators (reactive), the level of reduction of a target acoustic resonance was sensitive to room-mode damping. If the room mode was significantly damped, then there was little benefit in adding a lightly damped resonator. However, as resonator damping increased (becoming resistive), the sensitivity to mistuning was reduced. Another important point is that for constant resonator damping, the level of reduction of a target room mode increased as the damping of the room mode decreased. Therefore, high levels of reduction can only be achieved if the room mode is initially lightly damped. In such cases a resistive resonator may provide more optimal results than those for a reactive resonator. There is some inherent damping in acoustic resonators, which results from radiation losses and viscous effects in the neck. In the following tests, flow-resistive materials [paper mesh/filters used in convective coolers ("swamp coolers")] were inserted into the neck or tube sections to provide additional damping.

Test-Bed Development

The experiment used an external disturbance to excite internal acoustic modes through a lightly damped structural path, which is a good representation of the fairing problem. A rigid aluminum cylinder was used to provide a lightly damped acoustic volume. The longitudinal acoustic resonances of the cylinder are given by

$$f_n = c/\lambda_n \tag{6}$$

One end cap was made from medium-density particle board and approximated a rigid boundary condition. At the other end, a thin aluminum panel was attached, which provided a flexible structural transmission path. Although both boundary conditions were not rigid, the first three low-frequency acoustic modes were reasonably computed using

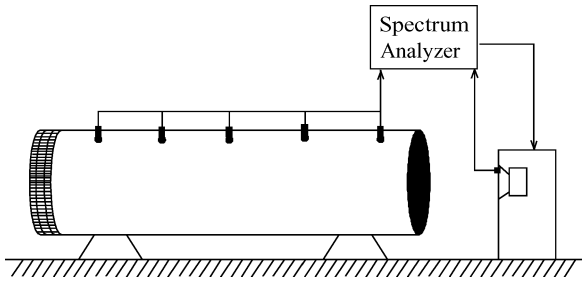

Fig. 9 Test bed used for experimental measurements.

$$\lambda_1 = 2L, \qquad \lambda_2 = L, \qquad \lambda_3 = 2L/3 \tag{7}$$

where L is the cylinder length. In subsequent frequency-response functions, it is easy to observe the lightly damped structural modes that resulted from the flexible aluminum panel.

The disturbance source was placed outside of the aluminum cylinder. If the source was placed inside of the cylinder, strong coupling between the speaker, the cylinder acoustic modes, and the resonators may have affected the measurements by impedance loading the disturbance. The tube resonators were effectively decoupled from the disturbance source, which prevented impedance loading of the disturbance. Microphones were mounted in the cylinder to measure the internal acoustic response.

Test Setup

A schematic of the test system is presented in Fig. 9. The test structure included an aluminum cylinder 2.1 m (7 ft) in length and 50 cm (20 in.) in diameter and with wall thickness of 7 mm (0.25 in.). (Uncertainty in these measurements was less than 1.6 mm.) One end cap was constructed from medium-density particle board with a thickness of 5 cm (2 in.). The other end cap was a thin aluminum panel with a thickness of 1.5 mm (1/16 in.). (The uncertainty in this measurement was less than 0.1 mm.) The first three acoustic resonances were predicted by Eqs. (6) and (7) to be 80, 160, and 240 Hz. The actual acoustic resonances were measured by placing a small (12.7-cm) speaker (mounted in a sealed cabinet) inside the chamber and measuring the frequency response from a microphone to an accelerometer attached to the speaker diaphragm with a spectrum analyzer. Measurements show that these resonances were 79, 161, and 241 Hz (uncertainty less than 0.5 Hz). The first few structural resonances of the aluminum panel were measured using an accelerometer and an impact hammer and were determined to be at 112, 213, and 220 Hz (uncertainty less than 0.5 Hz). Instrument-grade microphones were mounted inside the cylinder to measure the performance of the resonators. A 20.3-cm (8-in.) loudspeaker (woofer) in a sealed cabinet was positioned 0.5 m from the aluminum panel and used as the disturbance source. An accelerometer was placed on the diaphragm of the loudspeaker to provide a reference signal for measuring frequency-response functions (FRFs). This technique effectively removed the dynamics of the loudspeaker from the FRF measurements. A Siglab spectrum analyzer was used to generate random noise inputs for the speaker and to measure the microphone responses.

Results

Many tests were conducted to characterize the performance of the tube resonators. These tests included single and multiple resonator tests, analysis of neck position with acoustic coupling, analysis of tube damping on acoustic coupling, and robustness to mistuning. Most tests were conducted using T-shaped tubes, but could just as well have been performed with L-shaped resonators or U-shaped resonators. The frequency response of the open-loop structural-acoustic system measured at an interior microphone relative to loudspeaker diaphragm motion is given in Fig. 10. The first three acoustic

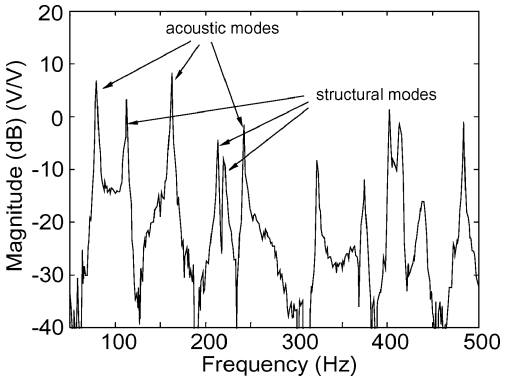

Fig. 10 Open-loop acoustic response at a single microphone.

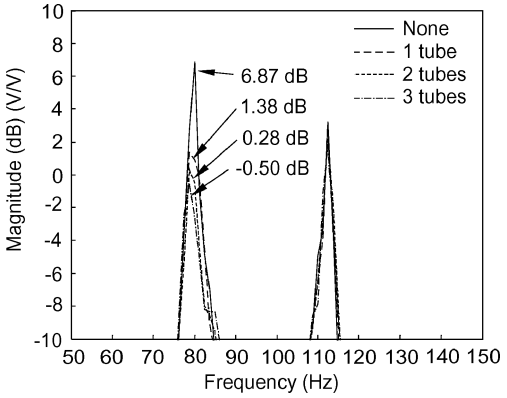

Fig. 11 Amplitude of the first acoustic mode using T-shaped resonators.

modes and the first three panel modes are indicated. Subsequent performance measurements presented in this paper used the same microphone location.

Figure 11 shows the effect on the amplitude response of the first acoustic mode for one resonator, two resonators, and three resonators added to the cylinder. In this case, T-shaped resonators were built [approximately 1.4 m (56 in.) in overall length] and placed within the cylinder on the end opposite the aluminum panel. A single resonator produced nearly 5.5 dB of reduction (narrow-band). A second resonator produced an additional 1.1 dB of reduction, and a third resonator added about 0.8 dB more for a total of 7.6 dB of reduction. (The measurement uncertainty of these measurements was less than 0.1 dB; the variation in subsequent measurements was less than ±0.2 dB.) In this test, no attempt was made to optimize resonator damping or to optimize the position of the neck in relation to the acoustic-pressure node. This test was intended to illustrate two important details. First, the resonators have a cumulative effect, but the benefits diminish with the number of resonators, which is consistent with Fahy's and Cummings's work. Second, a tube resonator much shorter than the overall cylinder can be used to target the fundamental cylinder mode, which is important from an applications point of view. In fact, an L-shaped resonator of much less length could have been used, which would have exhibited improved coupling because the neck could have been placed closer to the antinode of the acoustic mode.

The next test used three T-tube resonators for the second acoustic mode, and the measured response is given in Fig. 12. The "splitting of the peak" phenomenon discussed by Fahy and Schofield is illustrated in this plot. The data show that the amplitude of the resonant response was reduced by about 13.8 dB (±0.2 dB) using three resonators. The resonators were positioned just inside the cylinder on the end opposite the aluminum panel. The performance of these resonators exceeded the performance of the previous resonators in part because of neck position relative to the antinode of the second acoustic mode. The combined performance of the resonators

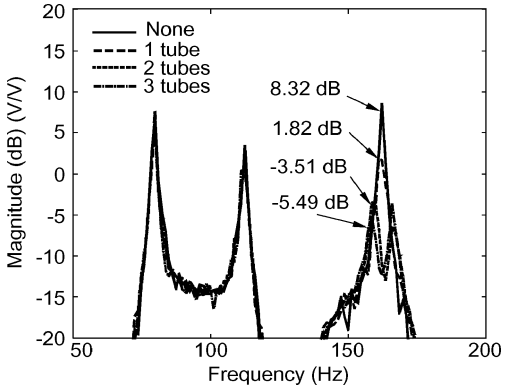

Fig. 12 Amplitude of the second acoustic mode using T-shaped resonators.

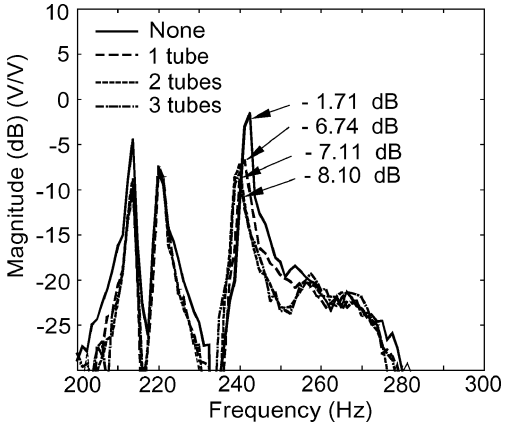

Fig. 13 Amplitude of the third acoustic mode using T-shaped resonators.

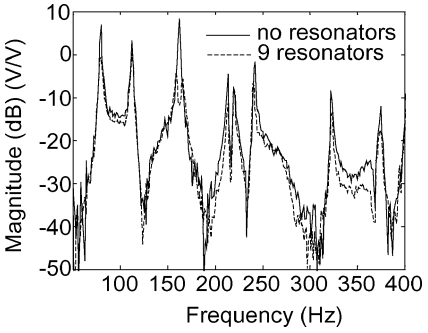

Fig. 14 Performance using nine T-shaped resonators, three for each of the first three acoustic resonances.

exceeded the individual performance, but less improvement was realized with each added resonator.

Figure 13 shows the performance of three T-shaped tube resonators designed for the third acoustic mode. The combined effect was approximately 6.4 dB (±0.2 dB) of reduction in the amplitude response. It is noteworthy that the tube resonators were able to couple with and attenuate the acoustic response by 3 to 4 dB at 212 Hz. This frequency corresponded to a bending mode of the aluminum-panel end cap, and was a significant noise-transmission path.

In the next test, nine T-shaped tube resonators were placed inside the cylinder around the circumference, three for each acoustic mode. The measured data are given in Fig. 14 with the frequency-response function of the empty cylinder (no resonators) superimposed. The amplitude response at almost all of the resonances, both structural and acoustic, was reduced. The resonators reduced the response of higher frequency resonances at 320 and 370 Hz as discussed

by Cummings. The reduction over the bandwidth (400 Hz) was computed to be 4.4 dB (±0.2 dB).

To improve the performance shown in Fig. 14, an attempt was made to optimize resonator coupling and resonator damping. First, flow-resistant material was placed in the long tube sections of the resonators. It was found that the damping could be controlled more precisely (gradually) if the flow-resistive material was placed in the tube sections as opposed to the neck, which is more commonly practiced. As flow-resistive material was added to the resonators, it produced different amounts of damping in each resonator design. This is illustrated in Fig. 15, which plots the reduction of the amplitude of the first three acoustic modes of the cylinder as a function of added material (measurement uncertainty less than 3 mm). In each case, a single tube resonator was placed at a consistent position within the cylinder and a frequency-response function measured. The reduction was computed as the ratio of the "no resonator" pressure amplitude, P_{nr}, to the pressure amplitude measured with the resonator, P_{res},

$$\text{reduction} = 20\log_{10}\left(\frac{|P_{\mathrm{nr}}|}{|P_{\mathrm{res}}|}\right) \tag{8}$$

A quadratic was curve-fitted to the data (in Matlab using double precision). The data show that there was an optimum damping treatment for each acoustic mode (experimental uncertainty was less than ±0.2 dB). This agrees with the theory developed by Fahy. (Note that the zero-damping reductions given in Fig. 15 are different from the reductions seen in previous data. This is entirely due to the position of the resonator within the cylinder, which will be addressed next.)

Next, the position of the neck relative to the pressure maxima of the acoustic wavelength was investigated for the first three acoustic modes and is shown in Figs. 16–18. In each of these tests, T-shaped resonators were used. The position of the center of the neck relative to the particle-board end cap is given normalized (i.e., divided) by the cylinder length (measurement uncertainty was less than 5 mm). The reduction was computed as the ratio of the amplitude response

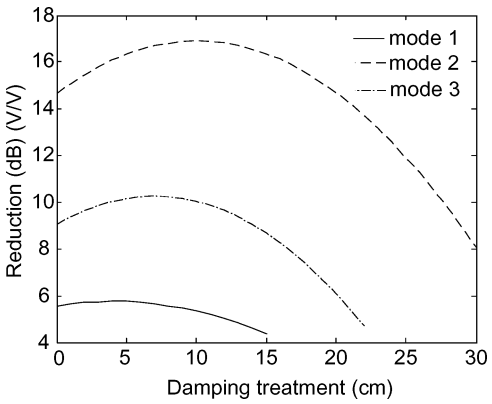

Fig. 15 Effect of added flow-resistive (acoustic damping) material on measured reduction of acoustic modes in the cylinder testbed.

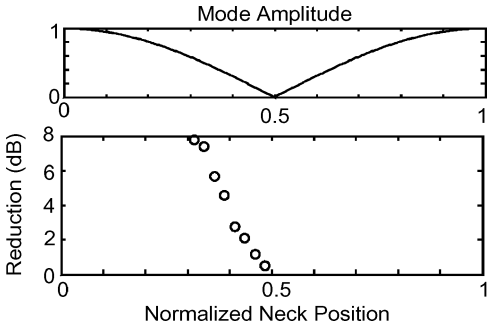

Fig. 16 Measured reduction of the first acoustic mode as a function of resonator neck position relative to the pressure node.

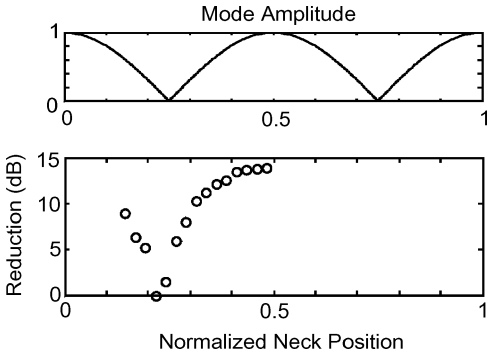

Fig. 17 Measured reduction of the second acoustic mode as a function of resonator neck position relative to the pressure node points.

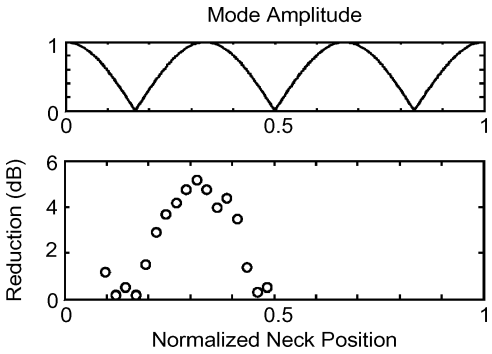

Fig. 18 Measured reduction of the third acoustic mode as a function of resonator neck position relative to the pressure node points.

of the acoustic resonance with no resonator, P_{nr}, to the amplitude response with a single resonator (undamped) at various positions, P_{res}, as given in Eq. (8).

Above the reduction plot is a plot of the amplitude of the acoustic mode shape along the cylinder. Figure 16 shows the measurements for the first (80-Hz) acoustic mode (again, the experimental uncertainty was measured to be less than 0.2 dB). As the neck approached the pressure node at the middle, the performance of the resonator decreased as expected. Figures 17 and 18 show the same phenomenon for the second and third acoustic modes. This demonstrates the importance of spatial coupling for resonator performance.

In the next test, nine resonators were placed in the cylinder. Three U-shaped resonators were used for the first mode to improve spatial coupling (the necks were placed near the pressure maximum), and T-shaped resonators were used for the second and third modes. Damping material was placed in all resonators in an attempt to improve damping. However, the damping treatments were based on previous single-tube measurements and an optimal solution was not sought iteratively. The resonator necks were positioned near antinodes for the particular acoustic modes. The results are given in Fig. 19 and show that a significant amount of attenuation was achieved at each of the targeted resonances, and considerable reduction was measured at higher frequencies. There was some, albeit less, attenuation at the panel resonant frequencies. The first and second acoustic modes were split, unlike the third, which exhibited a smooth plateau response. With further iterations, a more optimal damping treatment probably could be found for the first and second modes that would reduce the splitting effect. The reduction over the bandwidth was computed to 5.6 ± 0.2 dB, 2.2 dB more than in the previous test (Fig. 14). The U-shaped tubes produced significantly more reduction than the T-shaped tubes as a result of improved spatial coupling.

A final test was conducted to evaluate the robustness of resonator performance to frequency mistuning. A single resonator was designed for the first acoustic mode and the performance was computed as the frequency of the resonator was varied about the design frequency. In this test, a U-shaped tube was used, and the spatial location of the resonator was held constant. The performance was

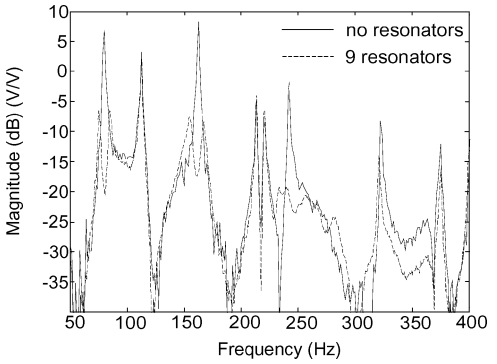

Fig. 19 Performance using three U-shaped resonators (first mode) and six T-shaped resonators (second and third modes).

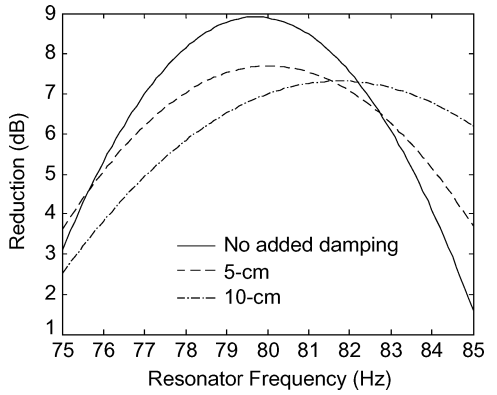

Fig. 20 Measured amplitude reduction of first acoustic mode as a function of resonator mistuning and damping treatment.

computed as the ratio of the amplitude of the acoustic resonance with no resonator, P_{nr}, to the amplitude of the acoustic resonance with the resonator, P_{res}, as given in Eq. (8). Data are shown in Fig. 20 for three different damping treatments, corresponding to no added material and 5 cm (2 in.) and 10 cm (4 in.) of added material (measurement uncertainty less than 3 mm). A quadratic curve was fitted to the data (in Matlab using double precision). A quadratic curve was chosen because it was the lowest-order polynomial function that seemed to fit the pattern indicated by the data. The data show that the lightly damped resonators can provide greater attenuation, but are more sensitive to mistuning than the damped resonators, which tended to have a flatter response curve indicating less sensitivity to mistuning. The measurements were repeated, and the experimental uncertainty was determined to be less than 0.2 dB.

Conclusions

A method for damping low-frequency acoustic resonances in composite Chamber Core payload fairings by using the fairing walls as long, tube-shaped acoustic resonators was presented and investigated. It was demonstrated that a relatively simple model for tube-shaped resonators of various geometries could be used to predict the first three resonances of the acoustic resonators. The tube resonators more closely followed quarter-wave resonators than classical lumped-mass Helmholtz resonators and were modeled with relatively few parameters. Experiments with T-shaped, L-shaped, and U-shaped resonators were performed and demonstrated that many of the conclusions developed by Fahy and Cummings in previous work with Helmholtz resonators and room acoustics are applicable to the tube-resonator/payload fairing problem presented here.

The effects of multiple resonators targeting multiple acoustic resonances were examined and showed that multiple resonators provided more attenuation and that a wider bandwidth of attenuation could be achieved by tuning the resonators to different frequencies. The importance of resonator damping and the spatial location of the resonator necks were investigated and showed that the performance of the acoustic resonators is strongly affected by both criteria. It was also observed that the resonators provided attenuation when their frequency did not exactly match the acoustic resonance, but that the robustness of the resonator to such mistuning was dependant upon damping. Resonators with more damping did not provide as much attenuation, but typically were more robust to frequency mistuning. Using three resonators in the test cylinder for a single mode attenuated the modal amplitude of the targeted mode by over 10 dB in the case of the first three acoustic resonances. It is expected that as the volume of the acoustic cavity increases, the number of resonators must also increase to achieve similar coupling. Nevertheless, the broadband reduction (0–400 Hz) achieved by using only nine resonators in the test cylinder was 5.6 dB ($\pm$0.2 dB), which likely could be improved with further iterations. The resonators coupled with and damped nearly all the acoustic resonances (and some peaks related to the structural transmission path) in the measured bandwidth. This is very promising for fairing noise control, where low-frequency acoustic resonances are problematic and not easily attenuated by acoustic-blanket treatments.

References

[1]Herup, E., Huybrechts, S., Griffin, S., and Tsai, S., "Method of Making Composite Chamber Core Sandwich-Type Structures with Inherent Acoustic Attenuation," U.S. Patent 6,231,710, filed, 2001.

[2]Henderson, K., Lane, S., Gerhart, C., and Richard, R., "Overview of the Vibro-acoustic Launch Protection Experiment at Air Force Research Laboratory," SPIE Smart Structures and Materials Conf., SPIE—The International Society for Optical Engineering, Bellingham, WA, March 2003.

[3]Beranek, L. (ed.), *Noise and Vibration Control*, Inst. of Noise Control Engineering, Washington, DC, 1988, pp. 362–376.

[4]Bies, D. A., and Hansen, C. H., *Engineering Noise Control*, E&FN Spon, New York, 1996, pp. 250, 349–353.

[5]Kuntz, H. L., Prydz, R. A., Balena F. J., and Gatineau, R. J., "Development and Testing of Cabin Sidewall Acoustic Resonators for the Reduction of Cabin Tone Levels in Propfan-Powered Aircraft," *Noise Control Engineering Journal*, Vol. 37, No. 3, 1991, pp. 129–142.

[6]Kinsler, L. E., Frey, A. R., Coppens, A. B., and Sanders, J. V., *Fundamentals of Acoustics*, 3rd ed., Wiley, New York, 1982, pp. 225–228.

[7]Chanaud, R. C., "Effects of Geometry on the Resonance Frequency of Helmholtz Resonators," *Journal of Sound and Vibration*, Vol. 178, No. 3, 1994, pp. 337–348.

[8]Selamet, A., Dickey, N., and Novak, J., "Theoretical, Computational and Experimental Investigation of Helmholtz Resonators with Fixed Volume: Lumped Versus Distributed Analysis," *Journal of Sound and Vibration*, Vol. 187, No. 2, 1995, pp. 358–367.

[9]Dickey, N., and Selamet, A., "Helmholtz Resonators: One-Dimensional Limit for Small Cavity Length-to-Diameter Ratios," *Journal of Sound and Vibration*, Vol. 195, No. 3, 1996, pp. 512–517.

[10]Li, D., and Vipperman, J., "Noise Control of a Cylinder Using Cylindrical Helmholtz Resonators," *Proceedings of IMECE 2003*, Paper IMECE03-41978, Fairfield, NJ, Nov. 2003.

[11]Schofield, C., *An Investigation into the Acoustic Interaction Between a Helmholtz Resonator and a Room*, Final-year B.Sc. Project Rept., Inst. of Sound and Vibration Research, Univ. of Southampton, Southampton, England, U.K., 1979.

[12]Fahy, F. J., and Schofield, C., "A Note on the Interaction Between a Helmholtz Resonator and an Acoustic Mode of an Enclosure," *Journal of Sound and Vibration*, Vol. 72, No. 3, 1980, pp. 365–378.

[13]Cummings, A., "The Effect of a Resonator Array on the Sound Field in a Cavity," *Journal of Sound and Vibration*, Vol. 154, No. 1, 1992, pp. 25–44.

L. Peterson
Associate Editor